

# Production of Helical Non-Neutral Plasmas by Collisionless Electron Penetration

HIMURA Haruhiko, WAKABAYASHI Hidenori, FUKAO Masayuki,  
ISOBE Mitsutaka<sup>1</sup>, OKAMURA Shoichi<sup>1</sup> and YAMADA Hiroshi<sup>1</sup>

*The University of Tokyo, Graduate School of Frontier Sciences, Tokyo 113-0033, Japan*

<sup>1</sup>*National Institute for Fusion Science, Toki 509-5292, Japan*

(Received: 9 December 2003 / Accepted: 11 March 2004)

## Abstract

For the first time, an experimental study on helical non-neutral plasmas (HNNP) has been performed on the Compact Helical System device. In order to produce HNNP, the collisionless penetration of electrons via the stochastic magnetic region (SMR) [H. Himura *et al.*, Phys. Plasmas **11**, 492 (2004)] is applied. The space potential ( $\phi_s$ ) is approximately limited by the initial potential of the injected electrons. The density of HNNP is about  $10^{11-13} \text{ m}^{-3}$  much smaller than the Brillouin density limit. The confinement time is inferred to be so far the order of 0.1 ms. From the first data, the equi-potential of HNNP seems to slightly deviate from the helical magnetic surface. When electrons are continuously injected into the SMR, the stable phase of HNNP continues only for 1–4 ms and then exhibits disruption with  $\sim 50$  kHz of oscillations. Data imply that the disruption is caused by an ion-related instability.

## Keywords:

helical non-neutral plasmas, electron penetration, stochastic magnetic region, Brillouin density limit, ion resonance instability

## 1. Introduction

There has been considerable interest both experimentally [1] and theoretically [2] in toroidal non-neutral plasmas, which are relevant to heavy ion accelerators [3], sources of highly stripped heavy ions [4], and thermonuclear fusion reactors [5]. These concepts are based totally on the electrostatic confinement of ions in a deep cavity of negative potential. For this purpose, a background cloud of magnetized electrons has been considered to be a candidate to form the negative well. Another significant feature of the background electrons is that a strong self-electric field  $E$  is intrinsically formed due to their space charge. This field could produce strong  $E \times B$  shear flow in a transverse magnetic field  $B$ . This property may be applied to confine two-fluid high- $\beta$  plasmas [6] which possess diamagnetic structures formed by the hydrodynamic pressure of the shear flow.

In order to produce such a toroidal non-neutral (pure electron) plasma, the source of the electrons should be placed outside closed magnetic surfaces. In axisymmetric (or two dimensional) toroidal geometry, several methods have been applied [7] to cause electrons across the magnetic surfaces and successful non-neutral plasmas have been generated. On the other hand, in non-axisymmetric (or three dimensional) geometry, no experimental studies have been performed until our recent work [8] in stellarator configurations on the

Compact Helical System (CHS) [9]. In the experiment, electrons are injected into the stochastic magnetic region (SMR) outside the last closed flux surface (LCFS), and for the case where the SMR is presented, some electrons penetrate quickly inside the LCFS. Consequently, they form helical non-neutral plasmas (HNNP).

In this paper, we briefly explain the first observation of HNNP produced by the method of collisionless electron penetration. In Sec. 2, we explain briefly the collisionless electron penetration on CHS. The first experimental data of HNNP are discussed in Sec. 3.

## 2. Helical electron plasmas produced by collisionless electron penetration

Experiments have been conducted on CHS. The machine is a medium-size stellarator device whose major ( $R$ ) and average radii ( $\bar{r}$ ) are 1.0 and 0.2 m, respectively. The key parameter which identifies the configuration is the magnetic axis ( $R_{ax}$ ) which is usually fixed at  $R = 101.6$  cm. For this case, the stochastic magnetic region (SMR) is present where the LCFS is completely detached from the vacuum chamber [8]. The typical magnetic field strength ( $B$ ) is 0.9 kG at  $R_{ax}$ , which yields  $\rho_e \sim 1.3$  mm when the maximum speed of electrons is assumed to be  $v_e \sim 2 \times 10^7$  m/s for  $eV_{acc} \sim 1.2$  keV,

where  $\rho_e$ ,  $v_e$ , and  $eV_{acc}$  are the Larmor radius, the electron velocity, and the beam energy, respectively.

Electrons are injected from a diode-type electron gun (henceforth called e-gun) which uses a LaB<sub>6</sub> emitter as the cathode. The LaB<sub>6</sub> cathode is quadrate (1.5 cm each) and the emitter has also a quadrille shape with tungsten wires. Values of beam current ( $I_b$ ) and  $eV_{acc}$  of the injected electrons can be varied. The e-gun is installed in the equatorial plane at  $z = 0$  and the cathode is placed in the SMR, usually at  $r \sim 117.5$  cm which is about 2 cm outside the LCFS. Nevertheless, substantial penetration of the injected electrons is observed in  $\sim 100$  ms. [8] and HNNP are produced inside the LCFS.

### 3. Properties of helical non-neutral plasmas

#### 3.1 Space potential (electron density)

As seen in Fig. 2 (b) of ref. [8], the profile of  $\phi_s$  (measured with a floating emissive probe [10]) achieves its maximum in the neighbor of  $R_{ax}$ . Figure 1 shows  $\phi_s$  at  $R_{ax}$  measured against  $eV_{acc}$  for cases of  $B = 0.9, 0.6,$  and  $0.3$  kG. As seen from the data,  $\phi_s$  increases significantly with  $V_{acc}$ . In addition, stronger  $B$  resulted in the larger  $\phi_s$ . This indicates that the maximum  $\phi_s$  is limited by both  $eV_{acc}$  and the strength of  $B$ . The dependence on  $eV_{acc}$  can roughly be understood by invoking energy conservation for the injected electron. Assuming rotational equilibrium [11] of HNNP with rotational speed  $= (-\nabla\phi_s)/B$ , then,  $e\phi_s = eV_{acc} - (3kT_e/2) - \omega P \leq eV_{acc}$  where  $(3kT_e/2) - \omega P \leq eV_{acc}$  and  $\omega P$  are thermal and rotation (flow) energies, respectively. On the other hand, the dependence on  $B$  is probably due to better confinement of electrons in the stronger  $B$ , not to an increased Brillouin density limit ( $n_B$ ) [11]. Since the value of  $\phi_s$  decreases monotonically, thus from the Poisson's equation ( $\nabla^2\phi = n_e e/\epsilon_0$ ), the experimental value of electron density ( $n_e$ ) is estimated to be  $10^{11-13} \text{ m}^{-3}$  for  $\phi_s \sim 1$  kV. On the other hand,  $n_B$  is calculated [1] to be  $\sim 10^{16} \text{ m}^{-3}$  for  $B = 0.9$  kG, too large to explain the observed  $n_e$ .

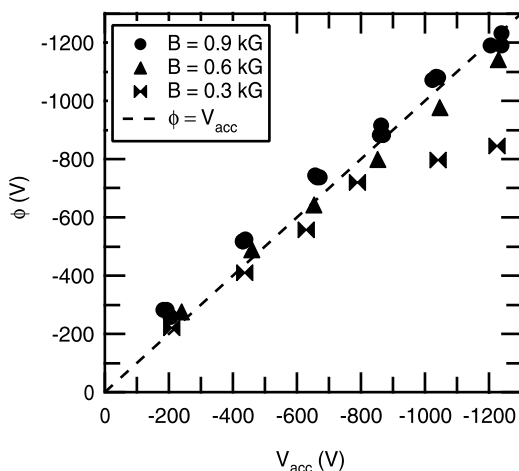


Fig. 1 The maximum  $\phi_s$ , which approximately reflects the value of electron density  $n_e$ , at the magnetic axis  $R_{ax}$  against the beam energy  $eV_{acc}$  for cases of  $B = 0.9, 0.6,$  and  $0.3$  kG. The dashed line shows  $\phi_s = V_{acc}$ . The data indicate that  $\phi_s$  is limited by  $eV_{acc}$ .

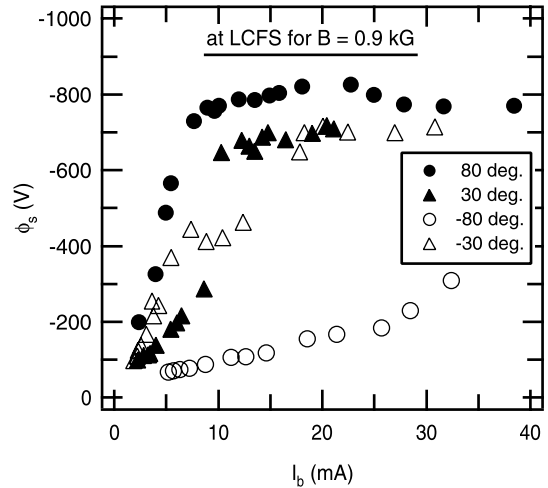


Fig. 2 Change in  $\phi_s$  for  $I_b$  for different pitch angles between  $B$  and  $v_e$ . Except for the case of  $-30$  deg.,  $\phi_s$  seems to saturate for  $I_b > \sim 10$  mA.

Figure 2 shows  $\phi_s$  taken from the  $r$ -probe [8] for the different pitch angle between  $B$  and  $v_e$ . As seen from the data, no change in saturation of  $\phi_s$  (density limitation) has been observed when the beam current  $I_b$  is increased, except for the case of  $-80$  deg. For  $I_b < 10$  mA,  $\phi_s$  increased almost linearly, however for  $I_b > 10$  mA,  $\phi_s$  saturated. This indicates that only a few more electrons drift inward across the LCFS with increased  $I_b$  and additional injected electrons are lost. Since  $n_e/n_B < 10^{-3}$ , the HNNP are categorized in strongly magnetized non-neutral plasmas [11]. Although further data is required, this implies that it may be hard to produce weakly magnetized HNNP ( $n_e/n_B \sim 1$ ). Regarding with the observed small fs for the case of  $-80$  deg., the reason is probably due to insufficient beam ejection caused by drift motion of thermionic electrons between the electrodes of the e-gun [12].

#### 3.2 Inferred confinement time

An estimate of the confinement time ( $\tau_N$ ) of HNNP can be obtained from the signal of the electrostatic probe ( $I_p$ ) placed at the LCFS. Typical data are shown in Fig. 3. It can be seen that  $I_p$  persists for 0.5–1 ms after the e-gun is turned off at  $t \sim 1.4$  ms. This suggests that  $\tau_N$  is about 0.5–1 ms. It should be noted that in most shots, a spike appears at the end of the duration of  $I_p$ , as seen at  $t \sim 3$  ms in Fig. 3. This might be the signal of a terminative disruption of HNNP.

Since  $\tau_N$  is order 0.1 ms, the transport coefficient in experiments ( $D_{exp}$ ) is calculated to be  $D_{exp} \sim \bar{r}^2/2\tau_N \sim 10^2 \text{ m}^2/\text{s}$ . The detail is now investigated. It should be noted that although in most neutral helical plasmas, the dominant transport mechanism is helically trapped particle (HTP) loss [13]. HTP does not account for HNNP. This is because the speed of HTP ( $v_h$ ) can be estimated as  $: m_e v_e^2 / (eBR_h) \sim 3 \times 10^4 \text{ m/s}$  where  $R_h$  is the radius of curvature for  $B$ . Thus, the coefficient ( $D_h$ ) due to the HTP loss is approximately  $\sim 10^6 \text{ m}^2/\text{s}$ , which is too large to explain  $D_{exp}$ . On the contrary, the coefficient ( $D_E$ ) due to radial electric field [13] is about  $D_E \sim 10$

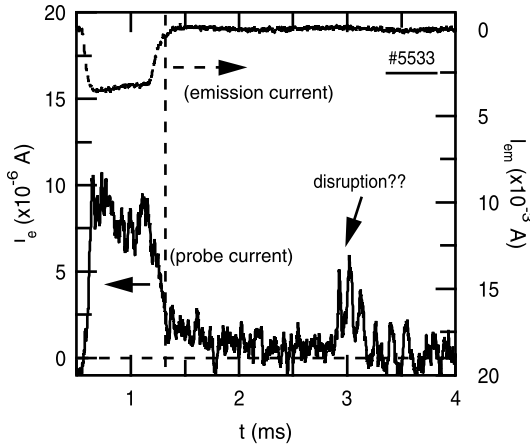


Fig. 3 Typical signals of  $I_p$  measured at the LCFS and emission current,  $I_{em}$ . Although at  $t \sim 1.4$  ms the electron emission is completely turned off, the output from  $I_p$  continues for approximately 1 ms more, which implies  $\tau_N \sim 1$  ms for this shot.

$\text{m}^2/\text{s}$ , which seems too small. Some other mechanism thus may govern the transport of HNNP.

### 3.3 Equi-potential surface

Since  $\phi_s$  has been measured at two different cross sections along the  $r$  and  $z$  axes, the location of the equi-potential surface can be compared with the helical magnetic surface. A typical data are shown in Fig. 4. As recognized, the equi-potential surface seems to deviate from the magnetic surface by  $\sim 0.1$  which is about 2 cm. Here, the banana width ( $Vr$ ) of a toroidally trapped particle does not explain the observed deviation;  $Vr$  can be estimated as  $2m_e v_{e\perp} \sqrt{R/\bar{r}}/B \sim 5$  mm. Here, it should be noted that the data in Fig. 4 is taken with keeping injection of electrons from the e-gun. Thus, further

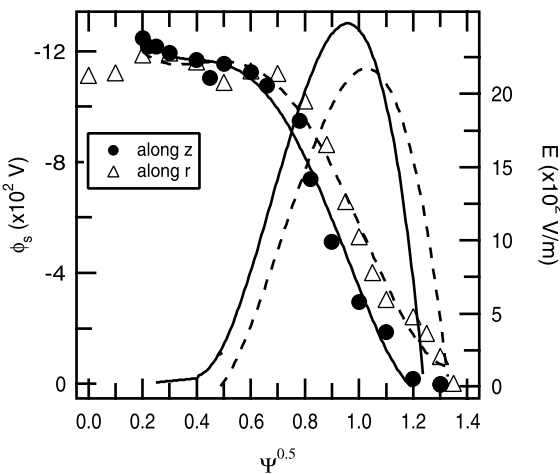


Fig. 4 Measured  $\phi_s$  along both  $r$  and  $z$  directions. Data are plotted for the normalized magnetic surfaces on which the LCFS is defined to be unity. Electric fields calculated from the fitting curves are also described. Data suggest that the equi-potential surface deviates from the helical magnetic surface by  $\sim 0.1$  that is about 2 cm.

measurements of  $\phi_s$  at other cross sections are required.

As recognized in Fig. 4, the value of  $E$  formed by the penetrated electrons is about 3 kV/m. This magnitude of  $E$  would produce an ion rotation velocity ( $E \times B$  speed) of  $\sim 10^5$  m/s in a neutral plasma for  $B \sim 0.9$  kG. However,  $E$  is formed only near the LCFS, which suggests the presence of few electrons around  $R_{ax}$  even in the possible equilibrium phase of HNNP.

### 3.4 Disruption

The stable phase described above lasts for 1–4 ms and then starts to disrupt. This event can be recognized from typical  $I_p$  data for different background pressure, shown in Fig. 5. Multiple disruptions are observed when electrons are continuously injected into the SMR. Evidence of the disruptions was also visible in the  $\phi_s$  signal. In experiments, we changed all other parameters ( $eV_{acc}$ , beam density  $n_b$ , and  $B$ ) and finally found out that the time interval between disruptions depends on the cross section for ionization of the background gas. The observed frequency of the disruption is about 50

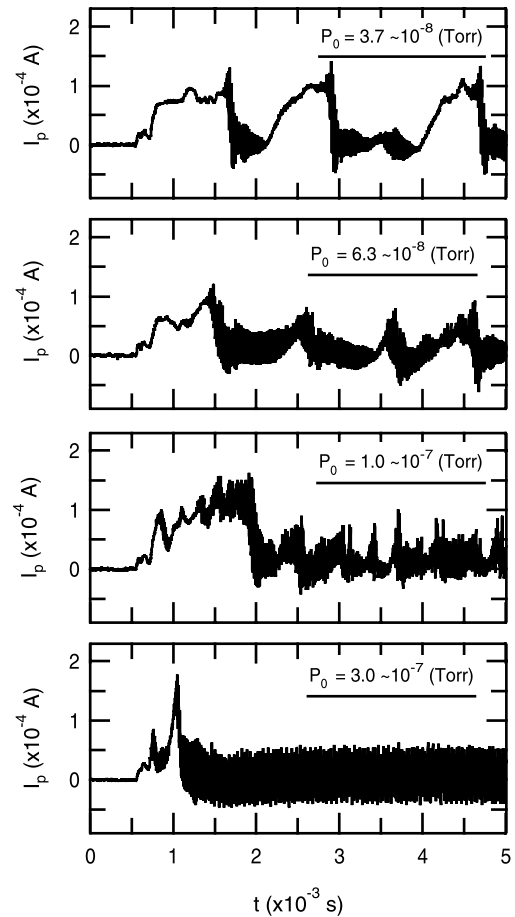


Fig. 5 A set of time evolutions of  $I_p$  at the LCFS for different background neutral pressure. Since the e-beam is continuously injected into the SMR, multiple disruption is induced. The time interval between disruptions strongly depends on the cross section for ionization of the background gas, suggesting an ion-related instability as a possible mechanism.

kHz and seems to be independent of the strength of  $B$ . The growth time of the disruption is about 50  $\mu$ s.

Although the details are still unknown, the above result strongly suggests that the e-beam ionizes the background gas and produces residual ions. Thus, some ion-related instability (IRI) may occur, driving both electrons and ions out of the closed magnetic surfaces. Assuming the conventional IRI [11] found in cylindrical systems occurs even in the helical geometry, a calculation of the  $m = 1$  mode agrees with the observed frequency and growth rates. Actually, the penetrated electrons must be ordered in drifting by  $E \times B$ . This implies that, even in the helically twisted magnetic field, a diocotron wave due to the drift motion could be generated because of the inhomogeneous  $B$  and  $E$ . If the residual ions start the slow rotation [11] and the ion angular velocity is different from the electron angular velocity, two-stream instability would be possible due to the differential rotation of electrons and ions. Once such instability is initiated, it would immediately grow in the neighborhood of  $R_{ax}$  because of the existence of rational surface ( $n = 2$  and  $m = 1$ ) for  $R_{ax} = 101.6$  cm. Furthermore, due to the small value of  $E$  around  $R_{ax}$ , little  $E \times B$  drift occurs, possibly resulting in little short-circuiting of perturbations in  $E$  due to the diocotron oscillation. Therefore, little suppression of the instability may occur around  $R_{ax}$  for the configuration where  $R_{ax} = 101.6$  cm. This hypothesis will be addressed in the second series of the

experiment.

## Acknowledgement

This research has been conducted since August, 2001 with the support and under the auspices of the NIFS LHD Project Research Collaboration.

## References

- [1] H. Himura *et al.*, Phys. Plasmas **8**, 4651 (2001).
- [2] S.M. Crooks *et al.*, Phys. Plasmas **3**, 2533 (1996).
- [3] G.S. Janes *et al.*, Phys. Rev. **145**, 925 (1966).
- [4] J.D. Daugherty *et al.*, Phys. Rev. Lett. **20**, 369 (1968).
- [5] T.H. Stix, Phys. Rev. Lett. **24**, 135 (1970).
- [6] H. Himura *et al.*, in *Fusion Energy 2000* (IAEA, Vienna, 2000) IAEA-CN-77-ICP/14.
- [7] C. Nakashima *et al.*, Phys. Rev. E **65**, 036409 (2002).
- [8] H. Himura *et al.*, Phys. Plasmas **11**, 492 (2004).
- [9] K. Matsuoka *et al.*, Plasma Phys. Control. Fusion **42**, 1145 (2000).
- [10] H. Himura *et al.*, Rev. Sci. Instrum. **74**, 4658 (2003).
- [11] R.C. Davidson, *Physics of Nonneutral Plasmas* (Addison-Wesley, Redwood City, 1990) p. 42.
- [12] H. Wakabayashi *et al.*, *to be submitted*.
- [13] M. Wakatani, *Stellarator and Heliotron Devices* (Oxford Univ. Press, New York, 1998) p. 271.